

SUPPORTING INFORMATION

Structural study of Calcium phosphonates: a combined synchrotron powder diffraction, solid-state NMR and first-principle calculations approach

S. Sene, B. Bouchevreau, C. Martineau, C. Gervais, C. Bonhomme, P. Gaveau, F. Mauri, S. Bégu, P. H. Mutin, M. E. Smith, and D. Laurencin

Supplementary Figures

Figure S1. IR spectra of Ca-phosphonate phases **1** to **5**.

Figure S2. TGA of Ca-phosphonate phases **1** to **5**.

Figure S3. SEM images of Ca-phosphonate phases **1** to **5**.

Figure S4. Whole pattern fitting plots (LeBail method) of the SPD diagrams of Ca-phosphonate phases **1** to **4**.

Figure S5. Simulated SPD patterns of Ca-phosphonate phases **1** to **4** (relaxed structures).

Figure S6. Different views of the crystal structures of Ca-phosphonate compounds **1** to **4**.

Figure S7. Comparison of Ca-binding modes of phenyl and butylphosphonate ligands, to those of phenyl and butylboronate ligands.

Figure S8. ^{31}P MAS NMR spectra of compounds **3** and **5**, recorded at a low spinning speed.

Figure S9. Evidence of preferential orientation of Ca-butylphosphonate crystallites in the rotor.

Figure S10. ^{13}C CPMAS NMR spectra of Ca-phosphonate phases **1** to **4**.

Figure S11. Comparison of ^{13}C NMR spectra of Ca-phosphonate phases **1** to **4**, recorded with (or without) ^{31}P decoupling during acquisition.

Figure S12. $^{13}\text{C}\{^{31}\text{P}\}$ REDOR NMR spectra recorded for phases **3** and **5**.

Figure S13. Natural abundance ^{43}Ca MAS NMR spectra of compounds **1**, **3** and **5**.

Figure S14. ^1H DUMBO NMR spectra of Ca-phosphonates **1** to **4**.

Figure S15. $^{31}\text{P}\{^{23}\text{Na}\}$ REDOR NMR study of **5**.

Figure S16. Evidence of $^3\text{J}_{\text{P-C}}$ couplings on ^{13}C NMR spectra of butylphosphonate phases **4** and **5**.

Supplementary Tables

Table S1. Experimental details for the acquisition of ^{31}P NMR spectra.

Table S2. Experimental details for the acquisition of ^{13}C NMR spectra.

Table S3. Experimental details for the acquisition of natural-abundance ^{43}Ca NMR spectra.

Table S4. Parameters used for whole pattern fitting plots (LeBail method) of the SPD diagrams of Ca-phosphonate phases **1** to **4**.

Table S5. Fractional atomic coordinates of Ca-phosphonates **1** to **4** after relaxation of all atomic positions.

Table S6. Experimental and calculated ^{31}P NMR parameters.

Table S7. Experimental and calculated ^{13}C isotropic chemical shifts.

Table S8. Experimental and calculated ^{43}Ca NMR parameters

Table S9. Experimental and calculated ^1H isotropic chemical shifts.

Figure S1. IR spectra of Ca-phosphonate phases **1** to **5**.

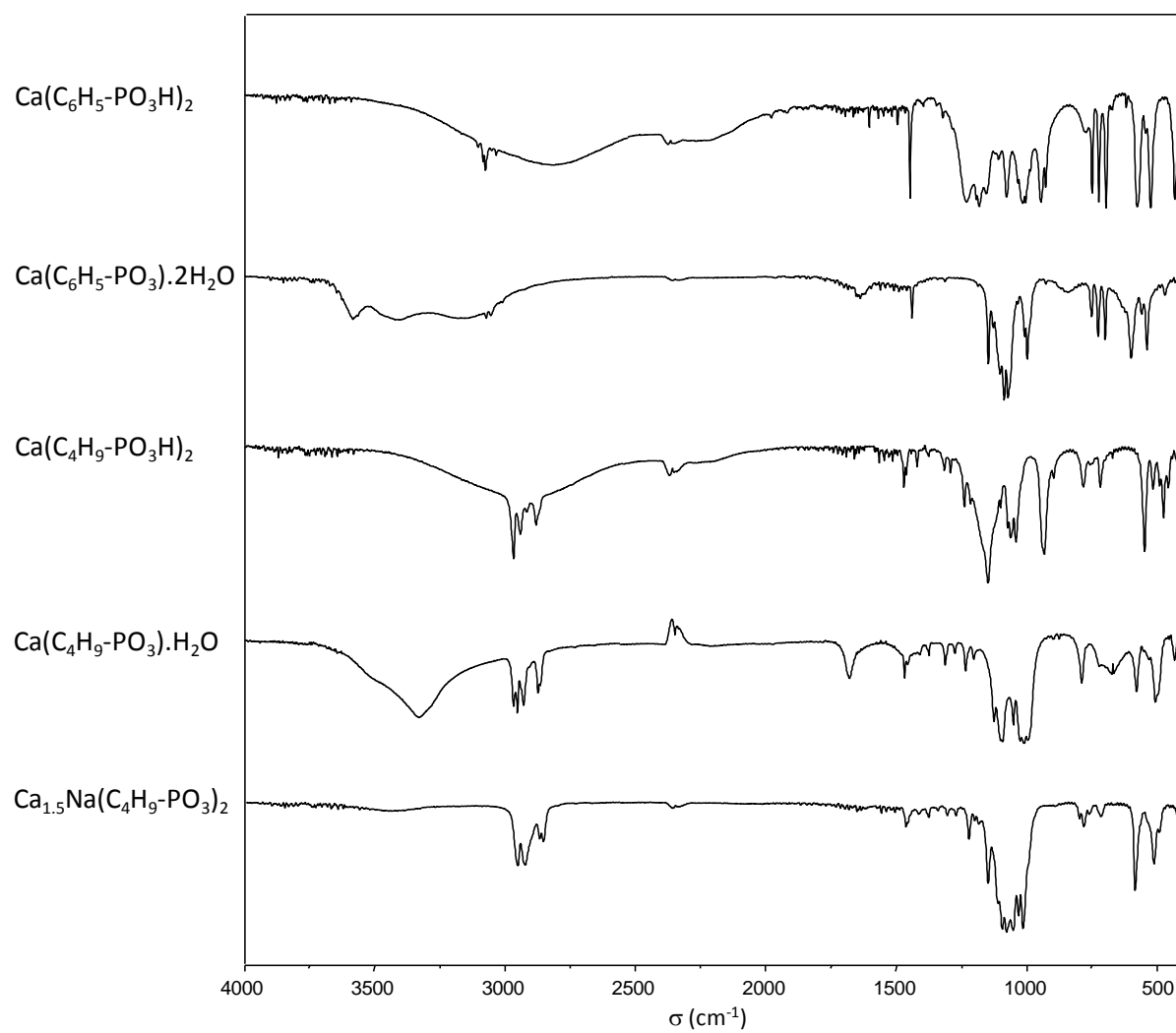


Figure S2. TGA of Ca-phosphonate phases 1 to 5.

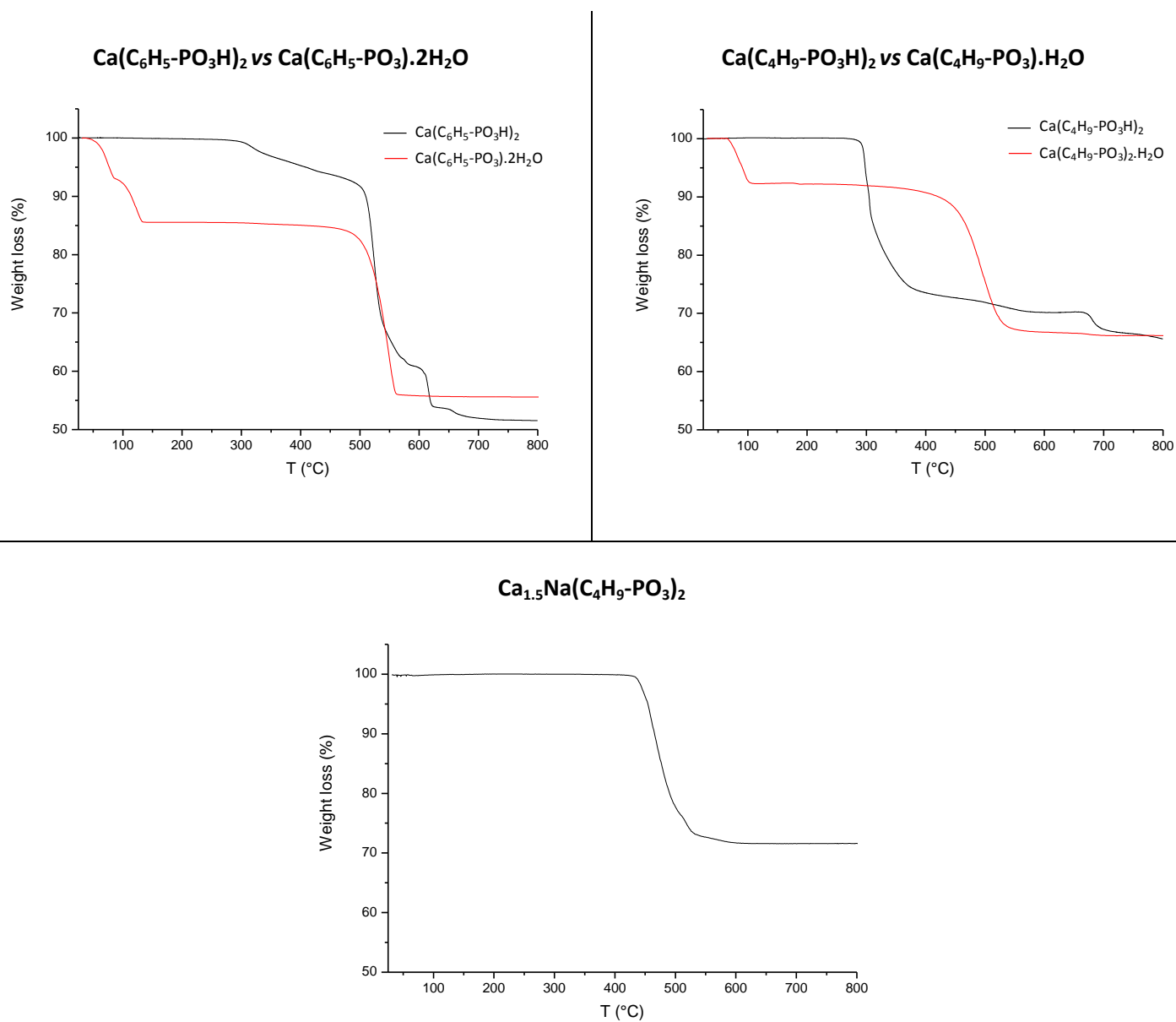


Figure S3. SEM images of Ca-phosphonate phases **1** to **5**.

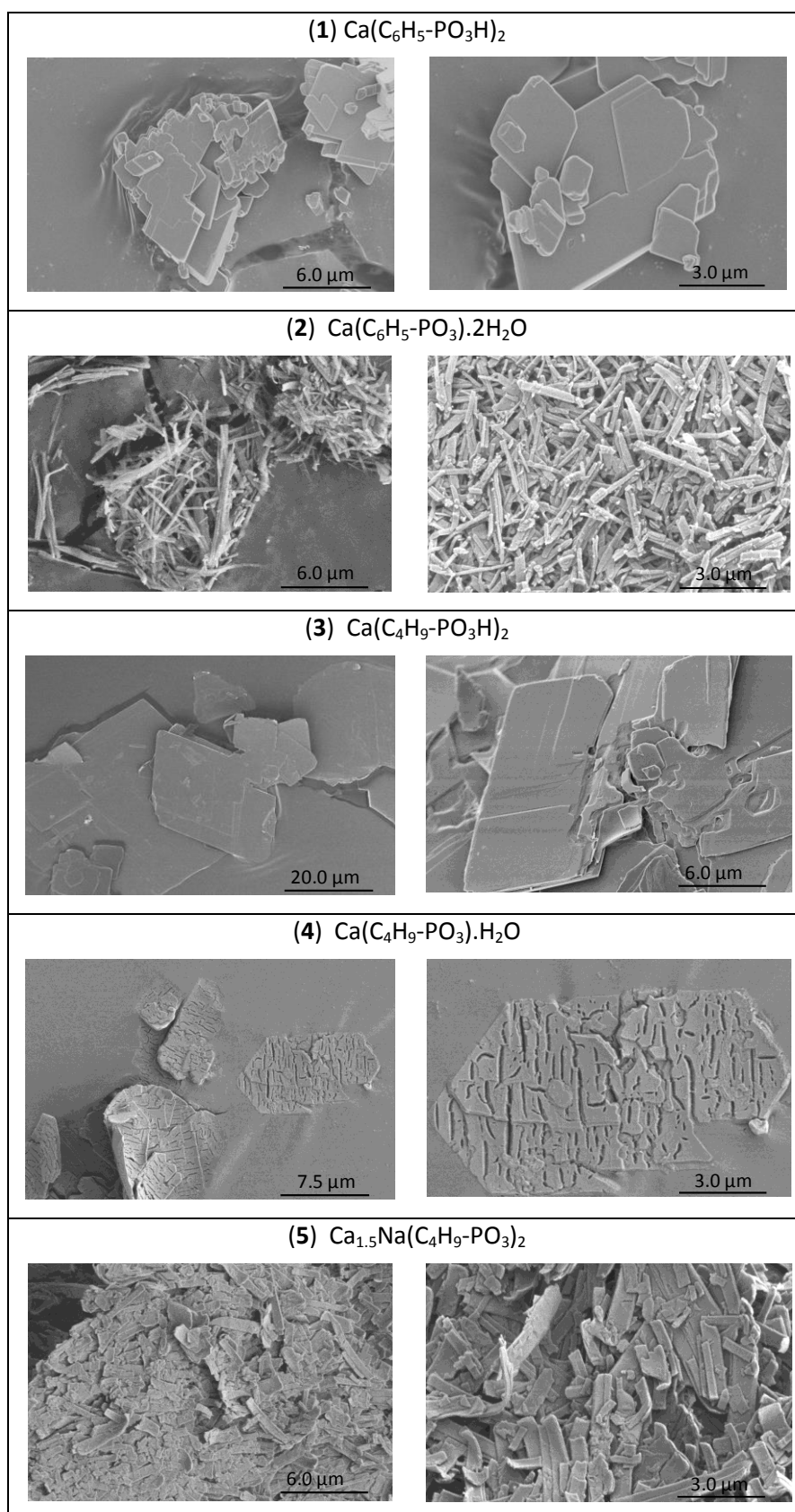


Figure S4. Whole pattern fitting plots (LeBail method) of the synchrotron powder diffraction diagrams of Ca-phosphonate phases **1** to **4**.

Vertical bars indicate the Bragg positions. Differences between experimental and calculated diagrams are shown below. Fit statistics are given in Table S4.

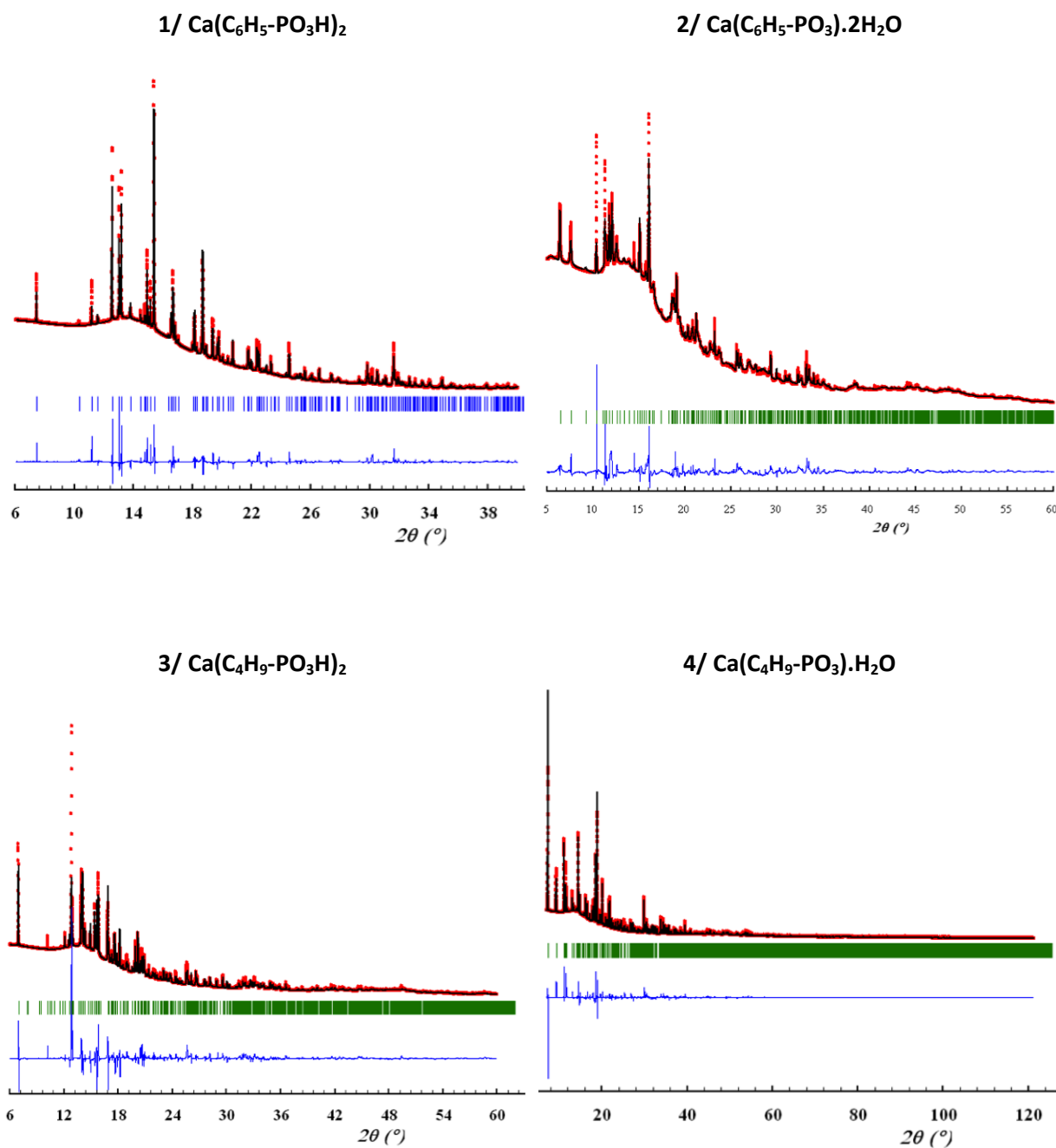


Figure S5. Simulated SPD patterns of Ca-phosphonate phases **1** to **4** (relaxed structures).

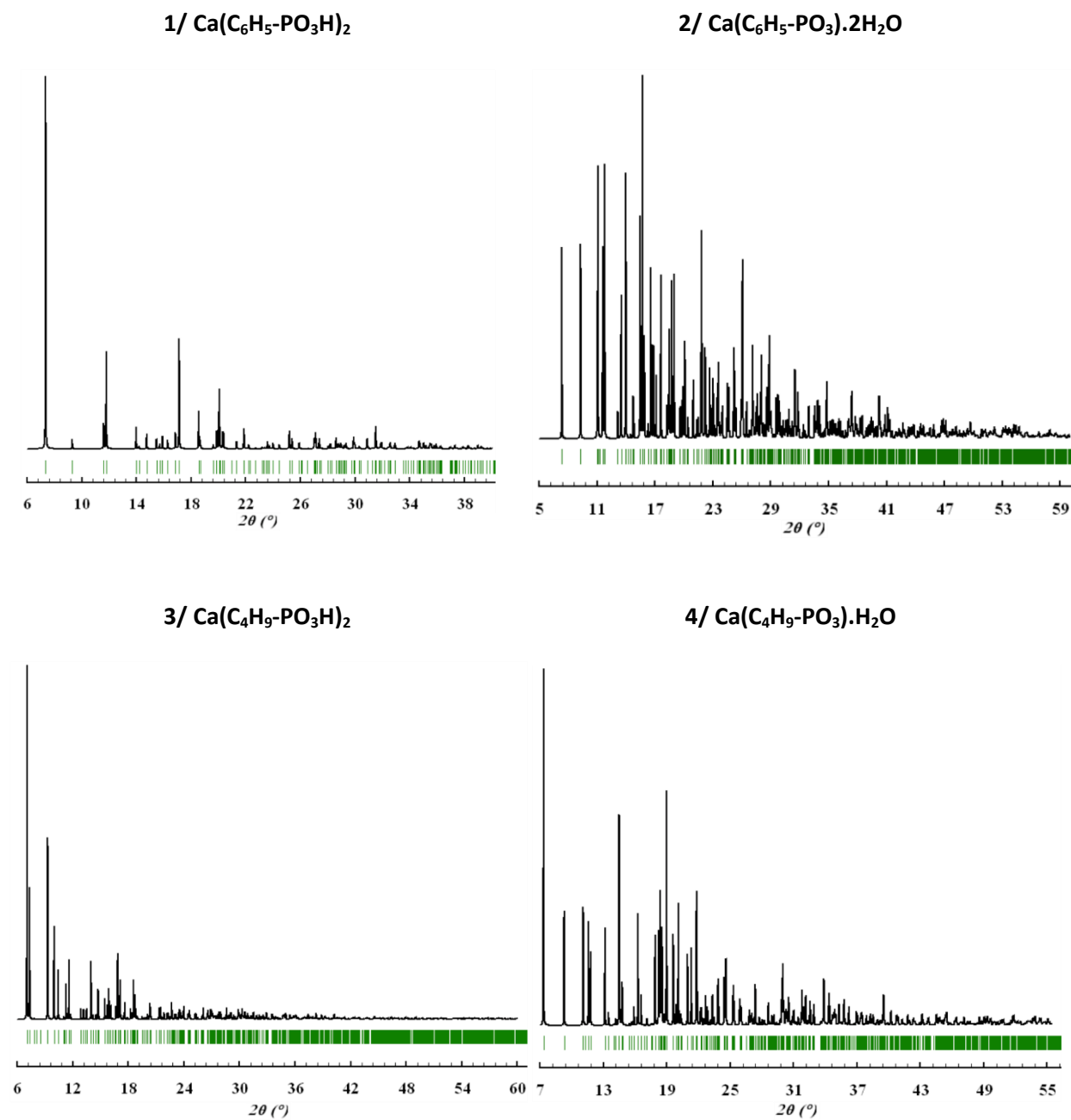


Figure S6. Different views of the crystal structures of Ca-phosphonate compounds **1** to **4**.

For each compound, the figure on the right represents an alternate view of the part of the structure shadowed in grey (looking in the direction of the arrow). Ca, P, C, O and H atoms are in green, black, grey, red, and white, respectively.

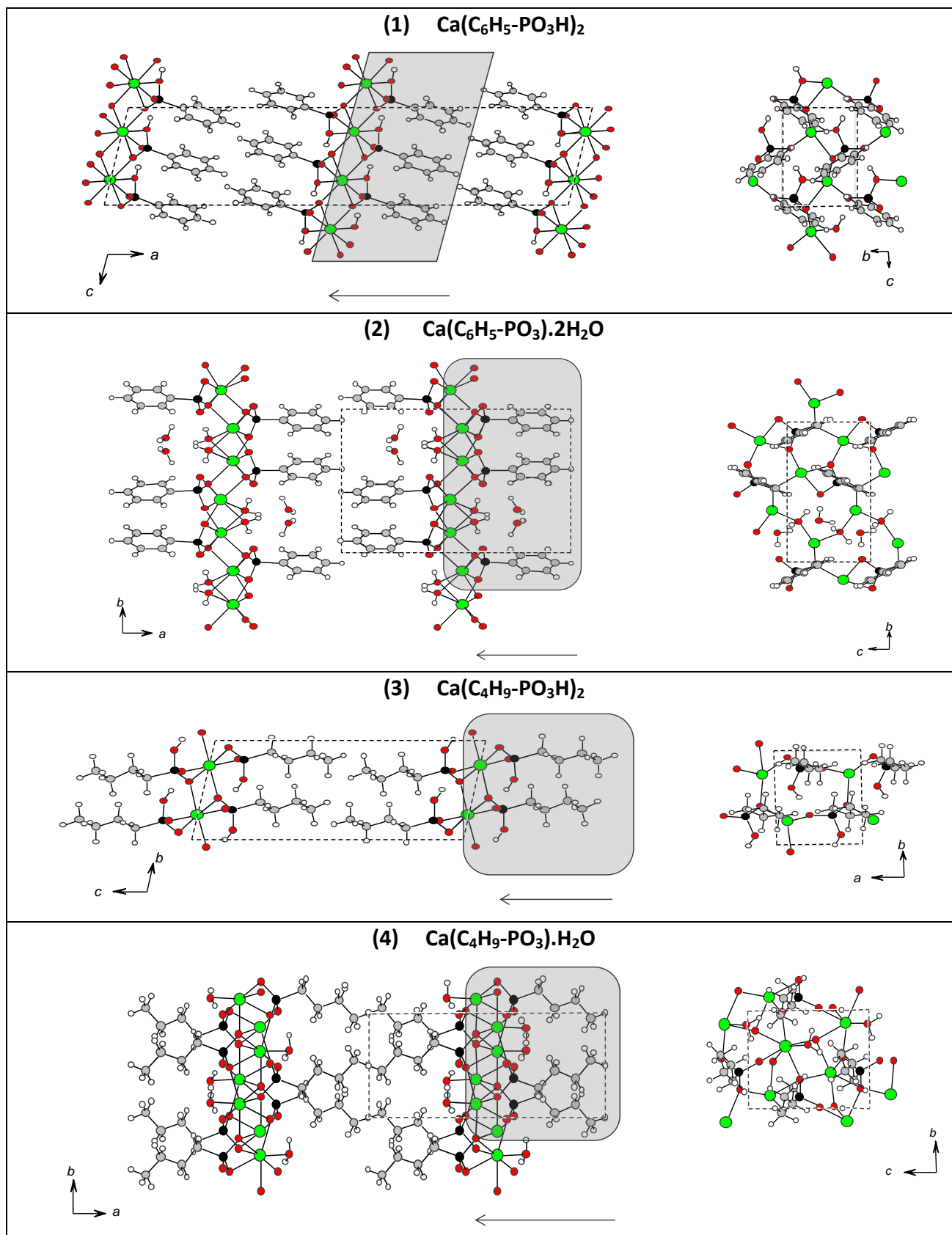


Figure S7. Comparison of Ca-binding modes of phenyl and butylphosphonate ligands, to those of phenyl and butylboronate ligands.

Ca, P, B, C, O and H atoms are in green, black, brown, grey, red, and white, respectively.

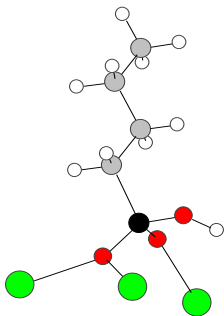
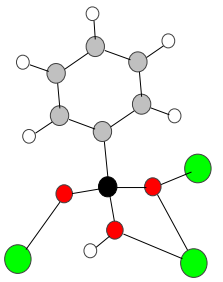
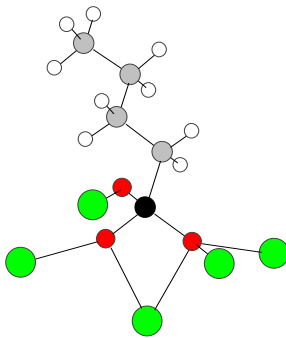
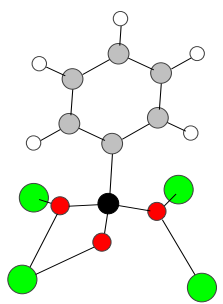
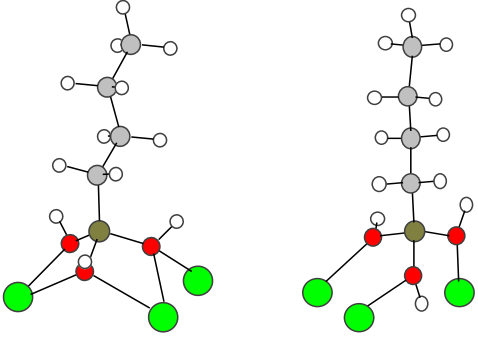
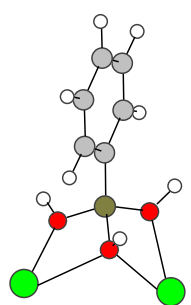
	Butyl- chain	Phenyl-chain
Phosphonate (R-PO₃H)	 <p>(1 Ca ; 2 Ca ; 1 H)</p>	 <p>(1 Ca ; 2 Ca ; 1 Ca + 1 H)</p>
Phosphonate (R-PO₃²⁻)	 <p>(1 Ca ; 2 Ca ; 3 Ca)</p>	 <p>(1 Ca ; 2 Ca ; 2 Ca)</p>
Boronate (R-B(OH)₃⁻)	 <p>(1 Ca ; 2 Ca ; 2 Ca) (1 Ca ; 1 Ca ; 1 Ca)</p>	 <p>(1 Ca ; 1 Ca ; 2 Ca)</p>

Figure S8. ^{31}P MAS NMR spectra of phases **3** and **5**, recorded at 9.4 T, at a low spinning frequency ($\nu_r \sim 1.6$ kHz). A fit is proposed for each spectrum, and the corresponding ^{31}P CSA parameters are reported above the spectra. Further details on the measurement conditions used to acquire the spectra can be found in Table S1.

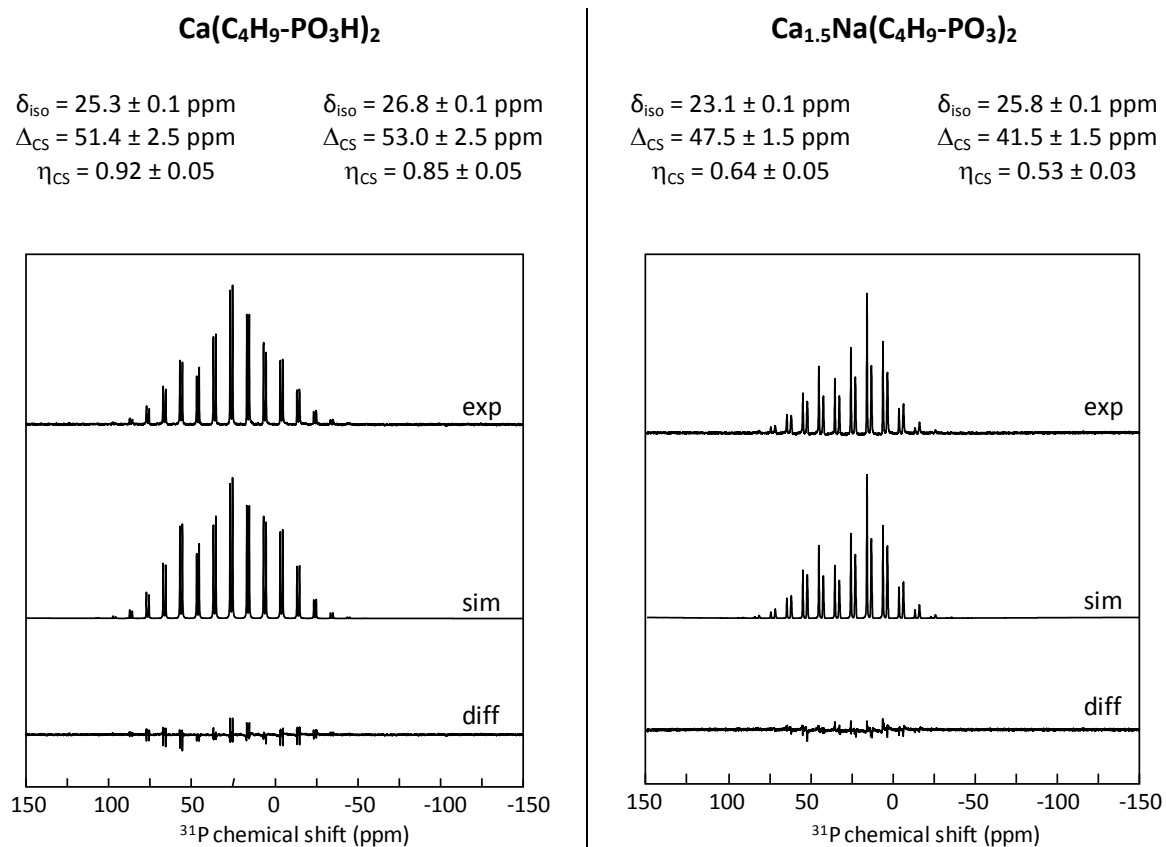


Figure S9. Evidence of preferential orientation of Ca-butylphosphonate crystallites in the rotor.

^{31}P static spectra of $\text{Ca}(\text{C}_4\text{H}_9\text{-PO}_3)\cdot\text{H}_2\text{O}$ (**4**), recorded at 9.4 T, either directly on the powder, or after diluting it physically in silica. In the latter case, a better agreement between experimental (solid line) and simulated lineshapes (dashed line) is observed.

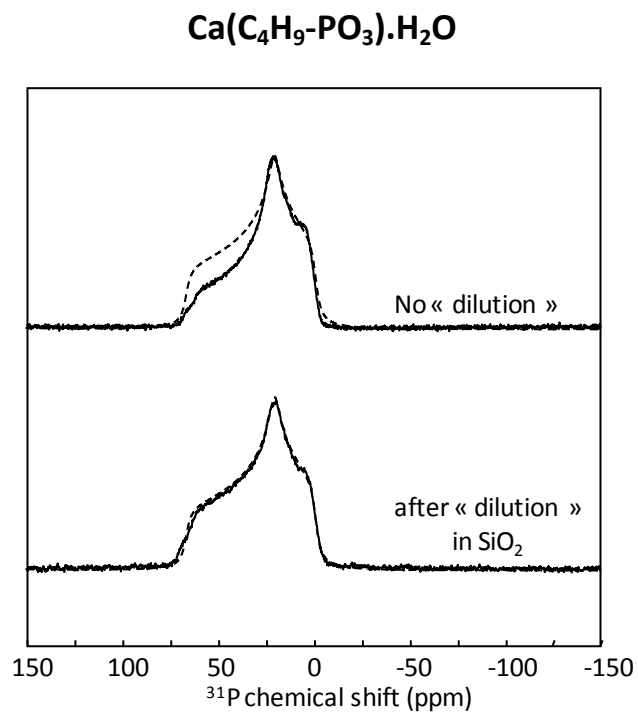


Figure S10. ^{13}C CPMAS NMR spectra of Ca-phosphonate phases **1** to **4**, recorded at 14.1 T (10 kHz MAS), without ^{31}P decoupling during acquisition. Further details on the experimental parameters used can be found in Table S2.

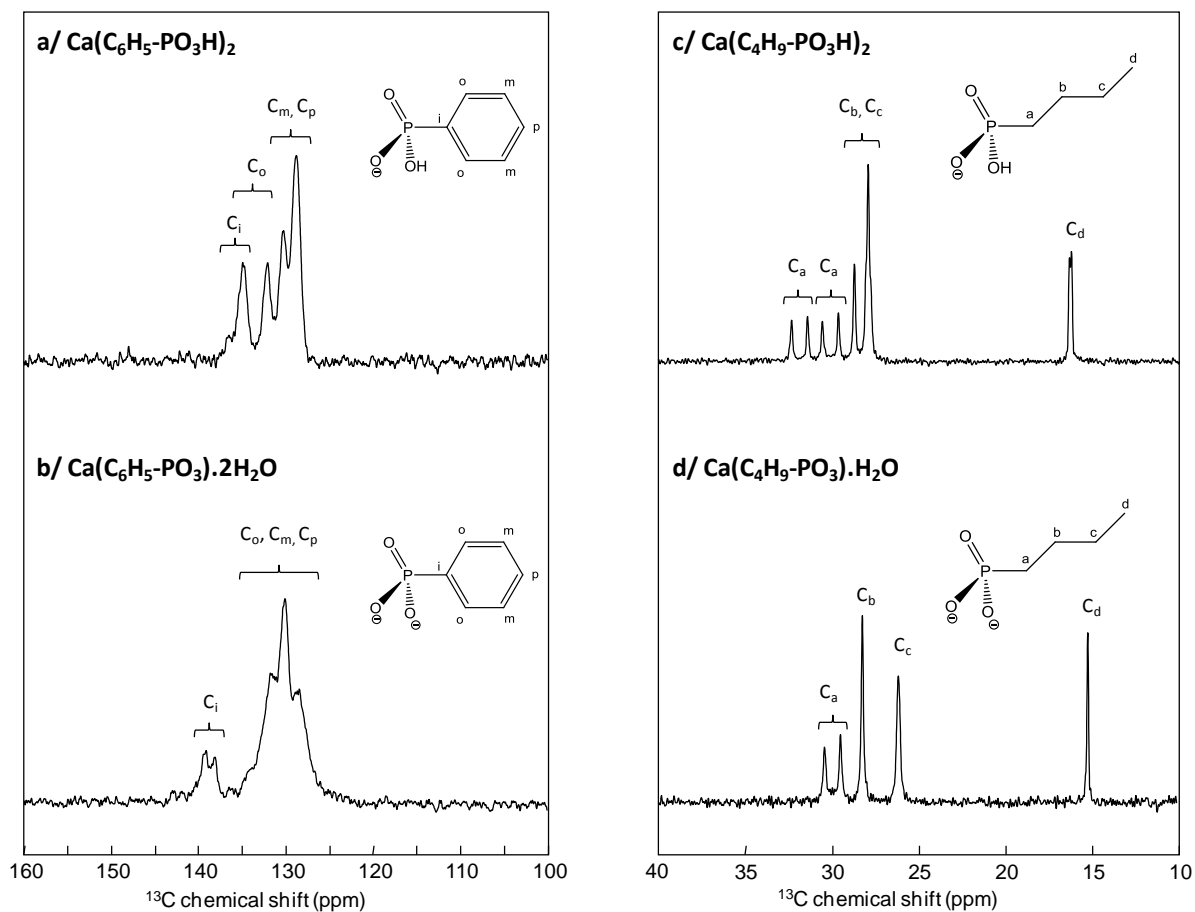


Figure S11. Comparison of ^{13}C NMR spectra of Ca-phosphonate phases **1** to **4**, recorded with (red) or without (black) ^{31}P decoupling during acquisition.

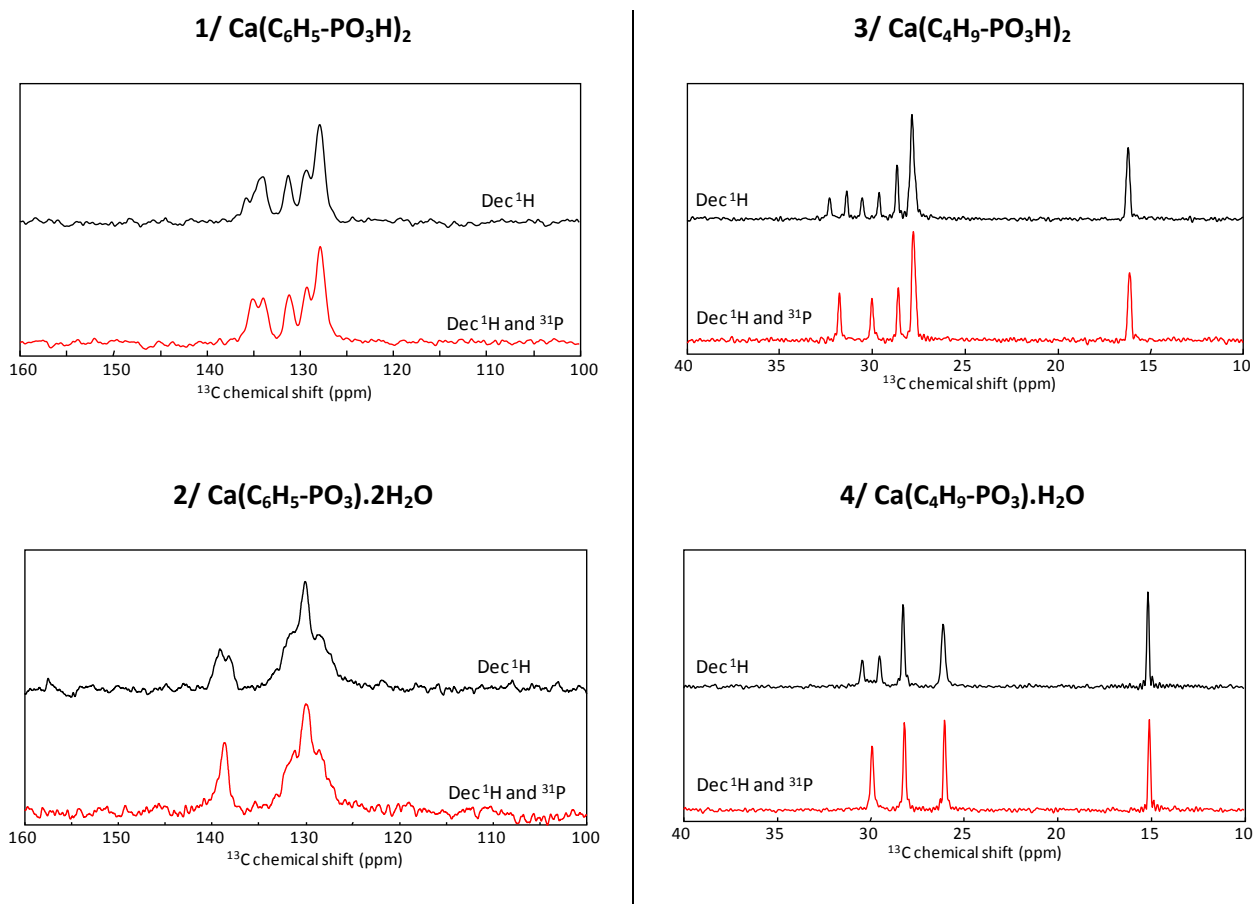


Figure S12. $^{13}\text{C}\{^{31}\text{P}\}$ REDOR NMR spectra recorded for phases **3** and **5**.

Details on the acquisition conditions can be found in the experimental section of the article. Spectra recorded with (red) and without (black) ^{31}P recoupling pulses were compared. The difference spectrum ΔS (grey) allows identification of the C atoms closest to the P.

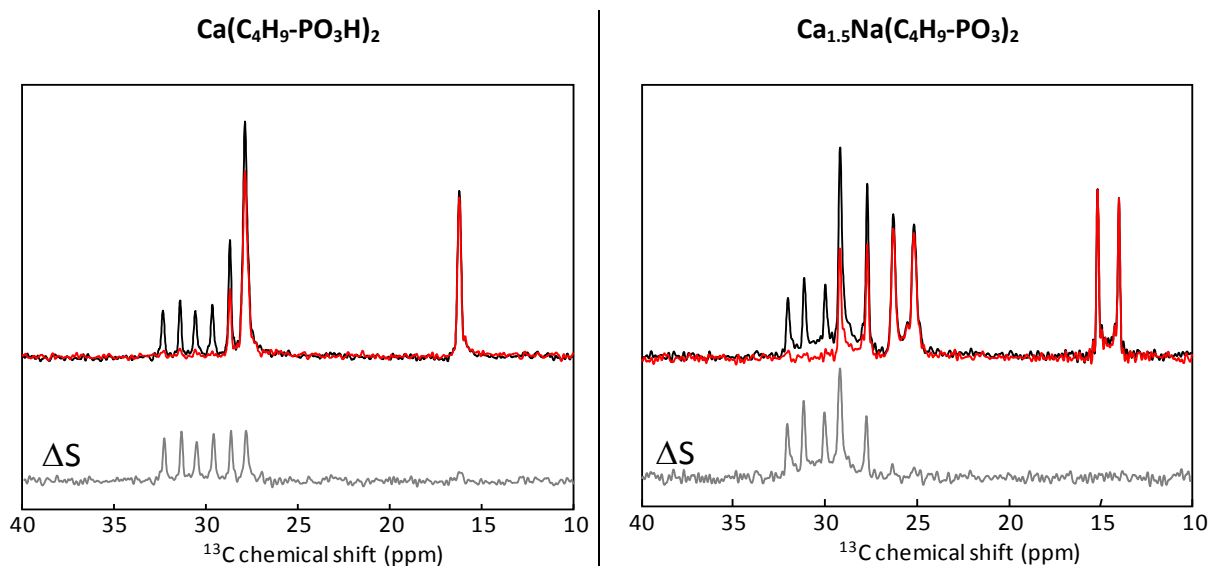


Figure S13. Natural abundance ^{43}Ca MAS NMR spectra of compounds **1**, **3**, and **5**.

Details on the acquisition conditions can be found in Table S3. Spectra were fitted at both fields (dashed red line) to extract the ^{43}Ca NMR parameters.

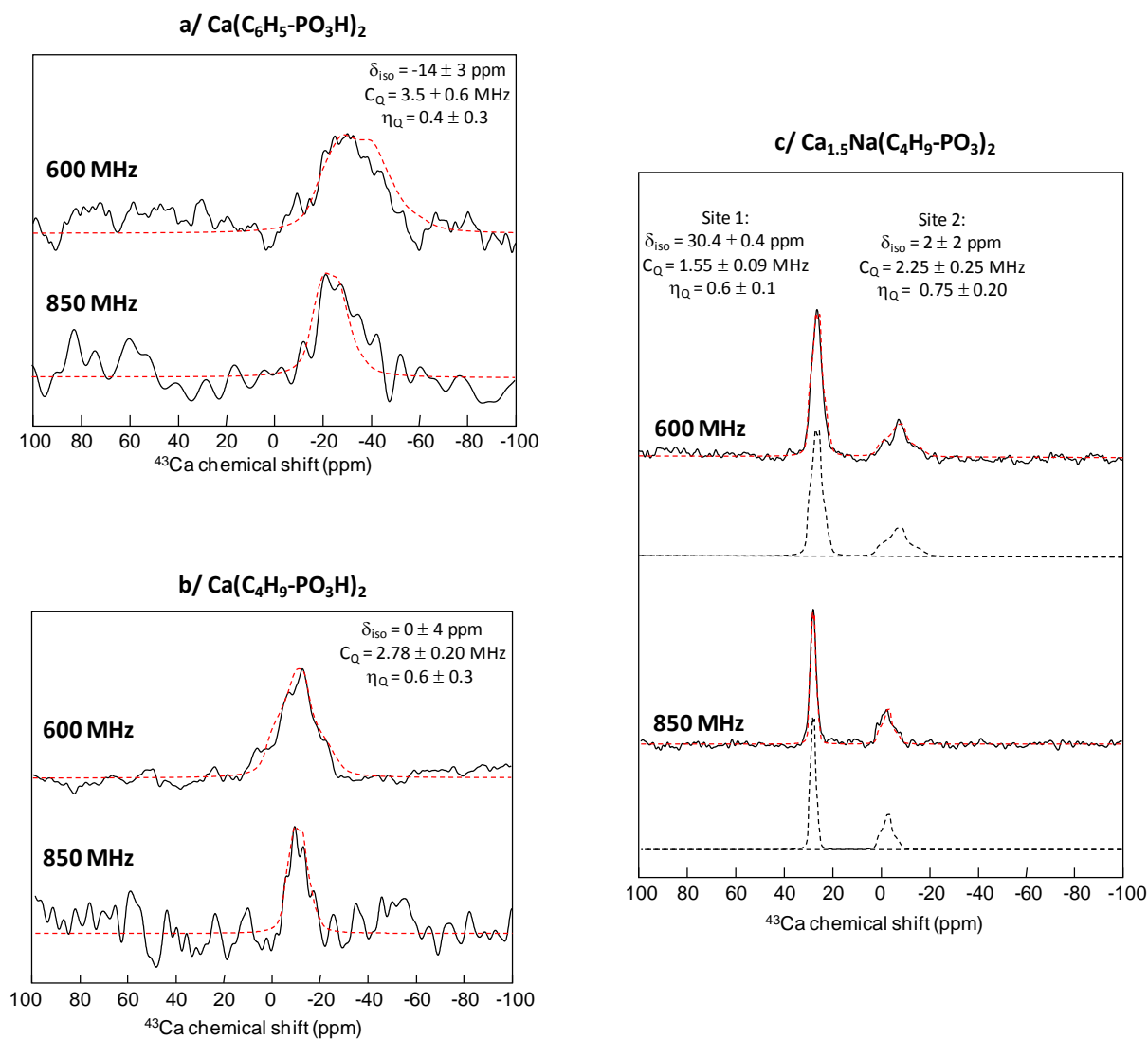


Figure S14. ^1H DUMBO NMR spectra of Ca-phosphonates **1** to **4**, recorded at 14.1 T, at 10 kHz MAS. Details on the acquisition conditions can be found in the experimental section of the manuscript. Artifacts due to the sequence used are indicated by (*) symbols on the spectra.

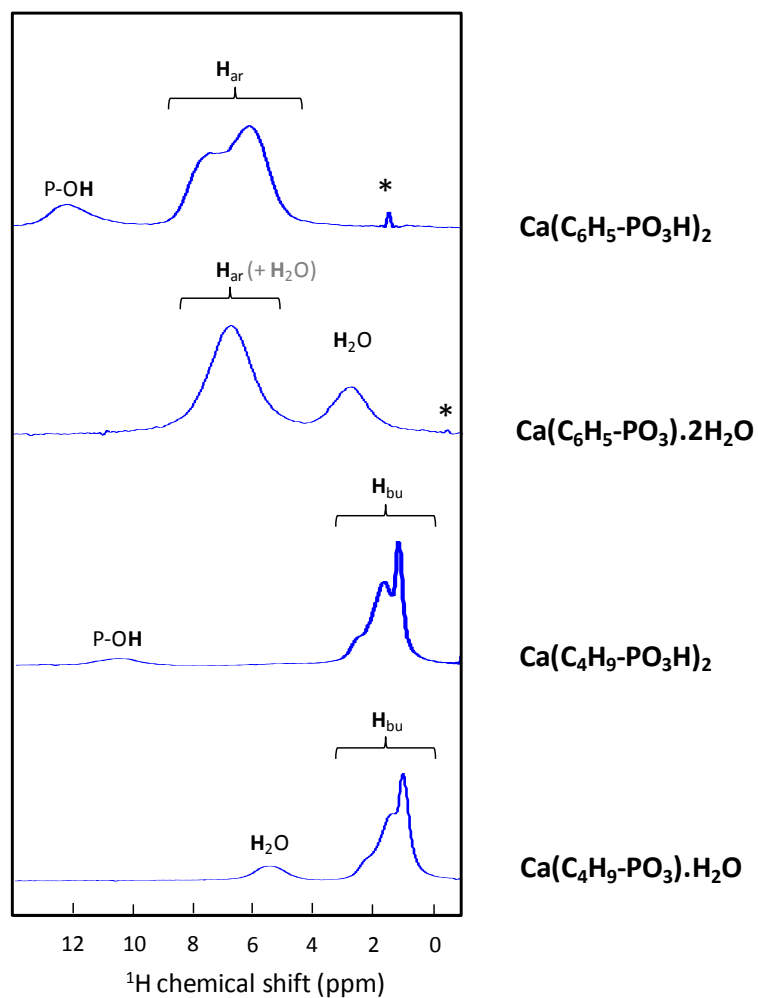
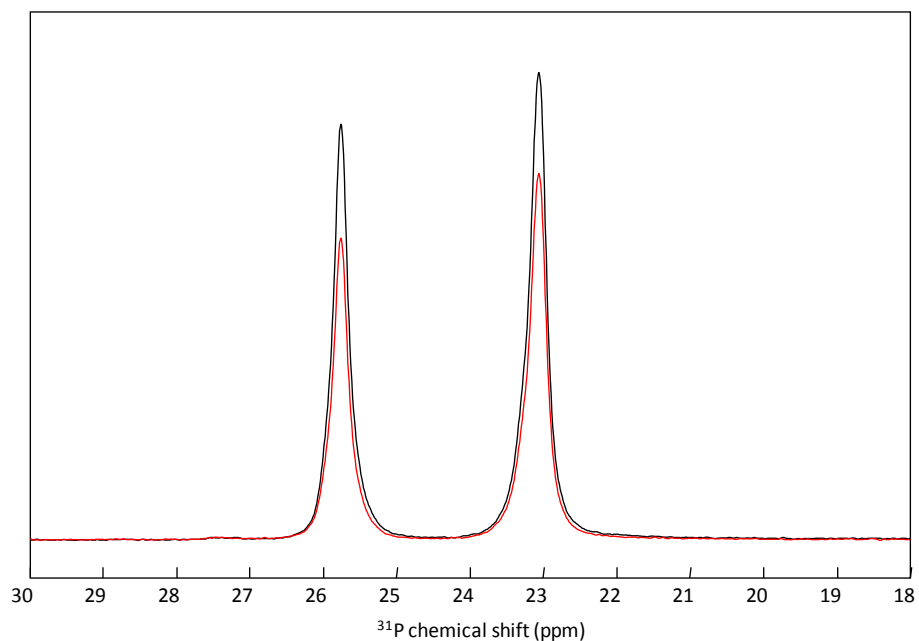


Figure S15. $^{31}\text{P}\{^{23}\text{Na}\}$ REDOR NMR study of **5**. Comparison of ^{31}P spectra recorded with (red) or without (black) ^{23}Na recoupling pulses.



The $^{31}\text{P}\{^{23}\text{Na}\}$ REDOR NMR experiment was carried out on the " $\text{Ca}_{1.5}\text{Na}(\text{C}_4\text{H}_9\text{-PO}_3)_2$ " phase, on a Varian VNMRS 600 MHz (14.1 T) spectrometer, using a 3.2 mm Varian T3 HXY MAS probe tuned to triple-resonance mode and spinning at 10 kHz. $^1\text{H} \rightarrow ^{31}\text{P}$ CP was first applied, with a $2.5 \mu\text{s}$ 90° ^1H excitation pulse, followed by a ramped contact pulse of 2 ms. A 3.2 ms total dephasing time was applied, with $6 \mu\text{s}$ rotor-synchronized 180° solid pulses on the ^{23}Na . The 180° pulse on the ^{31}P was $6 \mu\text{s}$. Spinal-64 ^1H decoupling (100 kHz RF) was used during the dephasing and acquisition periods. 8 transients were recorded, with a recycle delay of 16 s.

Figure S16. Evidence of $^3J_{P-C}$ couplings on ^{13}C NMR spectra of butylphosphonate phases **4** and **5**.

CPMAS NMR spectra recorded at 14.1 T, spinning at 20 kHz MAS. Further details on the acquisition conditions can be found in Table S2.

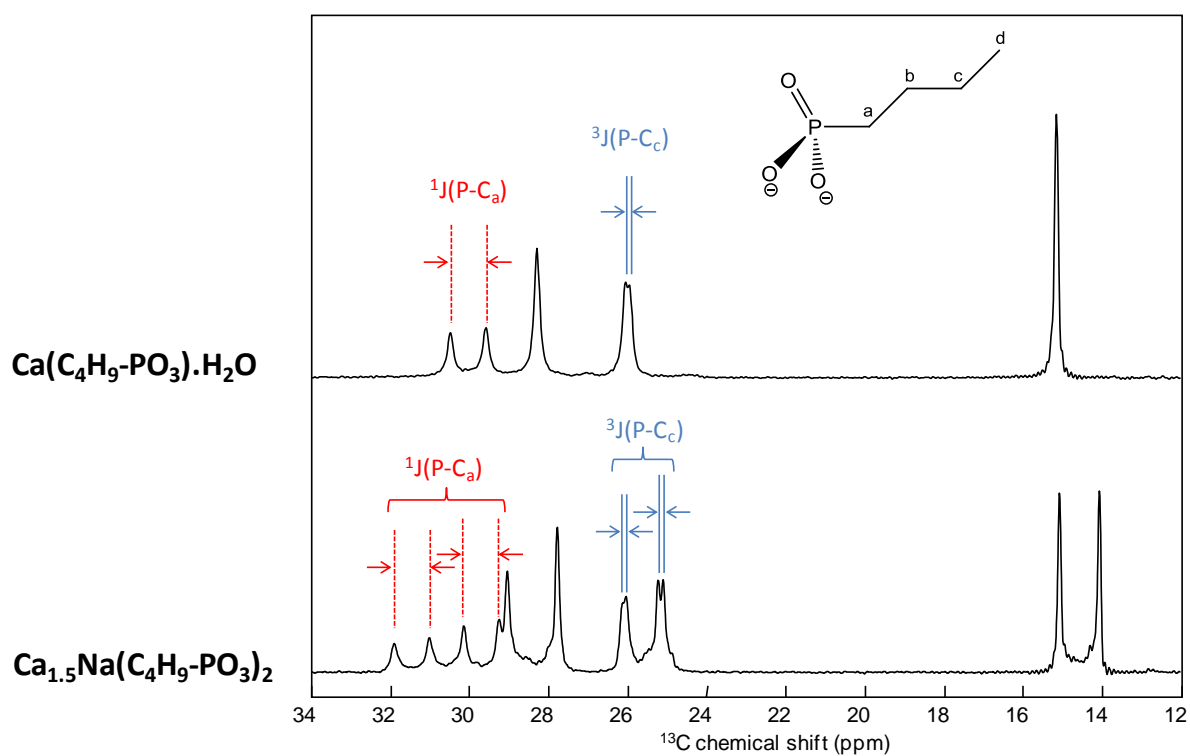


Table S1. Experimental details for the acquisition of ^{31}P NMR spectra.

	Field	MAS rate	Pulse sequence	D1	NS
Ca(C₆H₅-PO₃H)₂	9.4 T	20 kHz	Single pulse ^a	450 s ^b	8
	9.4 T	1.58 kHz	Single pulse ^a	450 s ^b	16
	9.4 T	Static	Hahn echo ^c	450 s ^b	184
	14.1 T	10 kHz	Single pulse ^d	450 s ^b	4
Ca(C₆H₅-PO₃)₂·2H₂O	9.4 T	20 kHz	Single pulse ^a	340 s ^b	4
	9.4 T	1.57 kHz	Single pulse ^a	340 s ^b	16
	9.4 T	Static	Hahn-echo ^c	340 s ^b	196
	14.1 T	20 kHz	CP ^e	16 s	4
Ca(C₄H₉-PO₃H)₂	9.4 T	20 kHz	Single pulse ^a	850 s ^b	4
	9.4 T	1.59 kHz	Single pulse ^a	850 s ^b	12
	9.4 T	Static	Hahn echo ^{c,f}	850 s ^b	184
	14.1 T	2.45 kHz	Single pulse ^d	850 s ^b	4
Ca(C₄H₉-PO₃)₂·H₂O	9.4 T	20 kHz	Single pulse ^a	160 s ^b	24
	9.4 T	1.56 kHz	Single pulse ^a	160 s ^b	12
	9.4 T	Static	Hahn echo ^{c,g}	160 s ^b	272
	14.1 T	20 kHz	CP ^e	16 s	4
Ca_{1.5}Na(C₄H₉-PO₃)₂	9.4 T	1.58 kHz	Single pulse ^a	400 s ^b	8
	14.1 T	Static	Hahn echo ^{h,i}	60 s	1728
	14.1 T	2.70 kHz	Single pulse ^d	400 s ^b	4
	14.1 T	20 kHz	CP ^e	16 s	4

^a Single pulse experiments were performed at 9.4 T using a 90° pulse of 5 μs on the ^{31}P , and 100 kHz spinal-64 ^1H decoupling during acquisition.

^b The recycle delay used allowed a full relaxation of the ^{31}P resonance.

^c Static Hahn echo experiments were performed at 9.4 T using a 90° pulse of 5 μs on the ^{31}P (180° pulse at 10 μs), an echo delay of 40 μs, and CW ^1H decoupling during acquisition (100 kHz RF).

^d Single pulse experiments were performed at 14.1 T using a 90° pulse of 3.25 μs on the ^{31}P , and 100 kHz spinal-64 ^1H decoupling during acquisition.

^e $^1\text{H} \rightarrow ^{31}\text{P}$ CPMAS experiments were performed at 14.1 T using a 2.5 μs ^1H 90° excitation pulse, followed by a 2 ms ramped contact pulse. Spinal-64 ^1H decoupling was applied during acquisition (100 kHz RF).

^f Preferential orientation of the crystallites in the rotor hampered the simulation of this static spectrum.

^g To avoid preferential orientation of the crystallites in the rotor, the powder was physically diluted in SiO₂ before recording the static spectrum.

^h Static Hahn echo experiments were performed at 14.1 T using a 90° pulse of 3 μs on the ^{31}P (180° pulse at 6 μs), an echo delay of 100 μs, and CW ^1H decoupling during acquisition (100 kHz RF).

ⁱ The static spectrum was difficult to simulate in this case, possibly due to (i) preferential orientation effects of the crystallites, (ii) ^{23}Na - ^{31}P dipolar couplings, and/or (iii) the choice of too short a recycle delay here.

Table S2. Experimental details for the acquisition of ^{13}C NMR spectra

	Field	MAS rate	Pulse sequence	D1	NS
Ca(C₆H₅-PO₃H)₂	14.1 T	10 kHz	CP ^{a,b}	20 s	256
		14 kHz	CP ^{a,c}	16 s	900
		10 kHz	CP-echo ^d	20 s	64
Ca(C₆H₅-PO₃)₂·2H₂O	14.1 T	20 kHz	CP ^a	8 s	5978
		10 kHz	CP ^{a,b}	3 s	1024
		10 kHz	CP-echo ^d	6 s	128
Ca(C₄H₉-PO₃H)₂	14.1 T	14 kHz	CP ^{a,c}	8 s	256
		10 kHz	CP ^{a,b}	6 s	48
		10 kHz	CP-echo ^d	6 s	16
Ca(C₄H₉-PO₃)₂·H₂O	14.1 T	20 kHz	CP ^a	8 s	312
		10 kHz	CP ^{a,b}	6 s	48
		10 kHz	CP-echo ^d	6 s	24
Ca_{1.5}Na(C₄H₉-PO₃)₂	14.1 T	20 kHz	CP ^a	8 s	312
		10 kHz	CP-echo ^d	6 s	32

^a CP experiments were recorded using a 2.5 μs 90° ^1H excitation pulse, followed by a 2 ms ramped contact time. Spinal-64 ^1H decoupling was applied during acquisition.

^b Temperature was regulated to +10 °C during the experiments at 10 kHz MAS.

^c These experiments were performed using a 4 mm MAS probe (while all others were recorded using a 3.2 mm MAS probe).

^d CP-echo experiments were recorded spinning at 10 kHz, using a rotor synchronized echo-delay of 100 μs (1 rotor period), a 2.5 μs 90° ^1H excitation pulse, a 3 ms ramped contact pulse, and an 8 μs 180° pulse on the ^{13}C . Spinal-64 ^1H decoupling (100 kHz RF) was applied during evolution and acquisition periods. Spectra were recorded both with and without spinal-64 ^{31}P decoupling during acquisition (100 kHz RF).

Table S3. Experimental details for the acquisition of natural abundance ^{43}Ca NMR spectra.

	Field	Probe rotor diameter	MAS rate	Pulse sequence ^{a,b}	D1	NS	Total expt time
Ca(C₆H₅-PO₃H)₂	14.1 T	9.5 mm	4 kHz	DFS-1pulse	7.0 s	36000	~70 h
	20.0 T	7 mm	4 kHz	RAPT-1pulse	1.0 s	47280	~13 h
Ca(C₆H₅-PO₃).2H₂O	14.1 T	9.5 mm	4 kHz	DFS-1pulse	0.8 s	89660	~20 h
	20.0 T	7 mm	4 kHz	RAPT-1pulse	0.8 s	32000	~7 h
Ca(C₄H₉-PO₃H)₂	14.1 T	9.5 mm	4 kHz	DFS-1pulse	1.5 s	52700	~22 h
	20.0 T	4 mm	5 kHz	RAPT-1pulse	0.8 s	140000	~31 h
Ca(C₄H₉-PO₃).H₂O	14.1 T	9.5 mm	4 kHz	DFS-1pulse	0.8 s	209300	~47 h
	20.0 T	7 mm	4 kHz	RAPT-1pulse	0.8 s	44000	~10 h
Ca_{1.5}Na(C₄H₉-PO₃)₂	14.1 T	9.5 mm	4 kHz	DFS-1pulse	0.8 s	103200	~23 h
	20.0 T	7 mm	4 kHz	RAPT-1pulse	0.8 s	49000	~11 h

^a DFS-1pulse conditions: convergence sweep from 400 to 80 kHz (duration ~ 6 ms; RF ~ 8 kHz); enhancement factor of ~2 (as tested on ^{43}Ca -labeled *CaHPO₄).

^b RAPT-1pulse conditions: set +X / -X 20 μs Gaussian pulses with ~150 kHz radiofrequency offset (RF ~ 9 kHz); enhancement factor ~2 (as tested on ^{43}Ca -labeled *CaHPO₄).

Table S4. Parameters used for whole pattern fitting plots (LeBail method) of the synchrotron powder diffraction diagrams of Ca-phosphonate phases **1** to **4**. Background was modeled manually.

	(1) Ca(C ₆ H ₅ -PO ₃ H) ₂	(2) Ca(C ₆ H ₅ -PO ₃).2H ₂ O	(3) Ca(C ₄ H ₉ -PO ₃ H) ₂	(4) Ca(C ₄ H ₉ -PO ₃).H ₂ O
No. FullProf profile	7 (TCH-pV)*	7 (TCH-pV)*	5 (pV)*	5 (pV)*
U	0.00021	0.0699	0.0079	0.0321
V	-0.00002	-0.0739	0	0
W	0.00006	0.0190	0.00321	0.00115
X	0.147	0.2406		
Y		0.1115		
Number of background pts	18	76	32	26
η (G/L mixing param.)			0.528	0.524
R _p (%)	19.6	21.7	26.7	17.6
R _{wp} (%)	21.5	20.4	30.0	16.9
R _{exp} (%)	2.89	2.77	5.97	2.90
χ ²	55.2	54.6	25.3	34.1

*TCH: Thompson Cox-Hastings; pV: pseudo-Voigt.

Spherical Harmonics coefficients for anisotropic size broadening for **(1)**

Y00	0.080	Y20	-0.096	Y22+	-0.184
Y22-	0.013	Y40	-0.267	Y42+	-0.206
Y42-	0.182	Y44+	0.109	Y44-	0.324

Spherical Harmonics coefficients for anisotropic size broadening for **(2)**

Y00	-2.37	Y20	-1.79	Y22+	-1.22
Y22-	-1.55	Y40	-0.29	Y42+	-0.66
Y42-	0.58	Y44+	-1.43	Y44-	1.01

Table S5. Fractional atomic coordinates of Ca-phosphonates **1**, **2**, **3** and **4** after relaxation of all atomic positions.

<i>Ca(C₆H₅-PO₃H)₂ (1)</i>				<i>Ca(C₆H₅-PO₃).2H₂O (2)</i>						
a = 31.4573 Å, b = 5.6432 Å, c = 7.7558 Å α = γ = 90°, β = 102.2347°				a = 15.0432 Å, b = 11.0379 Å, c = 5.7199 Å α = γ = 90°, β = 92.7490°						
Atom	x/a	y/b	z/c	Atom	x/a	y/b	z/c			
C1	0.3806	0.1970	0.9934	C5	0.7470	0.5769	0.3483			
C2	0.3506	0.0265	0.0231	C6	0.8040	0.6322	0.5178			
C3	0.2915	0.2677	0.8655	C7	0.7831	0.5234	0.1522			
C4	0.3212	0.4371	0.8345	C8	0.8955	0.6329	0.4920			
C5	0.3062	0.0625	0.9599	C9	0.8749	0.5236	0.1272			
C6	0.3656	0.4027	0.8988	C10	0.9311	0.5784	0.2969			
Ca17	0.5000	0.6080	0.2500	Ca16	0.4737	0.1338	0.6734			
H11	0.3619	0.8655	0.0947	H11	0.7768	0.6752	0.6697			
H12	0.2568	0.2958	0.8166	H12	0.7388	0.4819	0.0195			
H13	0.3102	0.5964	0.7596	H13	0.9393	0.6761	0.6236			
H14	0.2832	0.9297	0.9847	H14	0.9017	0.4815	0.9738			
H15	0.3888	0.5336	0.8737	H15	0.0027	0.5795	0.2784			
H16	0.4468	0.1882	0.3880	H19	0.7902	0.2198	0.9630			
O7	0.4637	0.3172	0.9822	H20	0.7400	0.1242	0.1069			
O8	0.4479	0.2712	0.2723	H21	0.6363	0.2365	0.4393			
O9	0.4484	0.8931	0.0848	H22	0.5938	0.1420	0.2610			
P10	0.4381	0.1578	0.0796	O1	0.5816	0.5256	0.1628			
<i>Ca(C₄H₉-PO₃H)₂ (3)</i>				O2				0.5959	0.6938	0.4726
a = 5.628 Å, b = 7.392 Å, c = 16.742 Å α = 101.228°, β = 87.673°, γ = 89.873°				O3				0.6154	0.4798	0.5973
Atom	x/a	y/b	z/c	O17				0.7680	0.2042	0.1181
C1	0.0473	0.6918	0.4148	O18				0.5795	0.2114	0.3647
C2	0.8645	0.6120	0.3532	P4				0.6287	0.5688	0.3931
C3	0.8631	0.7031	0.2785	<i>Ca(C₄H₉-PO₃).H₂O (4)</i>						
C4	0.6691	0.6223	0.2209	a = 15.5774 Å, b = 6.7082 Å, c = 8.1004 Å α = γ = 90°, β = 92.448°						
C9	0.4741	0.7953	0.5673	Atom	x/a	y/b	z/c			
C10	0.6509	0.8659	0.6326	C2	0.7204	0.2149	0.6231			
C11	0.5980	0.7946	0.7112	C3	0.7878	0.0480	0.6360			
C12	0.7555	0.8805	0.7806	C4	0.8762	0.1222	0.6980			
Ca17	0.8642	0.2531	0.0024	C5	0.9402	0.9519	0.7261			
H18	0.2285	0.6753	0.3876	Ca9	0.4566	0.1349	0.8161			
H19	0.0423	0.6228	0.4671	H11	0.7184	0.2990	0.7390			
H20	0.0162	0.8396	0.4380	H12	0.7374	0.3234	0.5288			
H21	0.6866	0.6254	0.3834	H13	0.7936	0.9764	0.5149			
H22	0.8969	0.4633	0.3328	H14	0.7669	0.9307	0.7199			
H23	0.0377	0.6848	0.2464	H15	0.8696	0.2051	0.8139			
H24	0.8345	0.8525	0.2981	H16	0.9011	0.2299	0.6094			
H25	0.4936	0.6546	0.2514	H17	0.9523	0.8742	0.6101			

H26	0.6855	0.4717	0.2061	H18	0.9151	0.8413	0.8119
H27	0.4748	0.6441	0.5522	H19	0.0020	0.0050	0.7786
H28	0.5139	0.8457	0.5110	H20	0.3525	0.4276	0.5968
H29	0.2923	0.8400	0.5885	H21	0.3348	0.2143	0.5322
H30	0.6472	0.0174	0.6460	O6	0.6158	0.0171	0.4056
H31	0.8329	0.8257	0.6093	O7	0.5859	0.9810	0.7122
H32	0.6183	0.6440	0.6986	O8	0.5462	0.2999	0.5658
H33	0.4108	0.8244	0.7304	O10	0.3335	0.3550	0.4957
H34	0.7385	0.0312	0.7933	P1	0.6125	0.1256	0.5722
H35	0.9444	0.8500	0.7646				
H36	0.6776	0.0048	0.1221				
H37	0.7209	0.5016	0.8804				
O6	0.8295	0.5839	0.0599				
O7	0.7536	0.9014	0.1440				
O8	0.3984	0.6878	0.0981				
O14	0.4289	0.8071	0.8977				
O15	0.8407	0.9250	0.9427				
O16	0.8080	0.6045	0.8602				
P5	0.6578	0.6964	0.1238				
P13	0.6968	0.8076	0.8767				

Table S6. Experimental and calculated ^{31}P NMR parameters.

Structure	Phosphonate Connectivity ^a	δ_{iso} (ppm)		Δ_{CS} (ppm) ^e		η_{CS} ^e		
		Exp ^{b,c}	Calc ^d	Exp ^{b,c}	Calc ^d	Exp ^{b,c}	Calc ^d	
$\text{Ca}(\text{C}_6\text{H}_5\text{-PO}_3\text{H})_2$	(1Ca; 2Ca; 1Ca+1H)	10.1 ± 0.1	17.6	-83.8 ± 1.5	-92.0	0.93 ± 0.02	0.92	
$\text{Ca}(\text{C}_6\text{H}_5\text{-PO}_3)_2 \cdot 2\text{H}_2\text{O}$	(1Ca; 2Ca; 2Ca)	12.5 ± 0.1	21.3	63.9 ± 1.5	66.6	0.42 ± 0.02	0.51	
$\text{Ca}(\text{C}_4\text{H}_9\text{-PO}_3\text{H})_2$	Site 1 (P5)	(1Ca; 2Ca; 1H)	25.3 ± 0.1	34.6	51.4 ± 2.5	57.1	0.92 ± 0.05	0.96
	Site 2 (P13)	(1Ca; 2Ca; 1H)	26.8 ± 0.1	38.5	53.0 ± 2.5	59.0	0.85 ± 0.05	0.84
$\text{Ca}(\text{C}_4\text{H}_9\text{-PO}_3)_2 \cdot \text{H}_2\text{O}$	(1Ca; 2Ca; 3Ca)	28.8 ± 0.1	40.2	37.3 ± 1.5	38.6	0.59 ± 0.05	0.46	
$\text{Ca}_{1.5}\text{Na}(\text{C}_4\text{H}_9\text{-PO}_3)_2$	Site 1		23.1 ± 0.1		47.5 ± 1.5		0.64 ± 0.05	
	Site 2		25.8 ± 0.1		41.5 ± 1.5		0.53 ± 0.03	
$\text{Ca}(\text{CH}_3\text{-PO}_3)_2 \cdot \text{H}_2\text{O}$ ^f	(1Ca; 2Ca; 3Ca)		38.7		39.0		0.53	
$\text{Ca}(\text{C}_6\text{H}_{13}\text{-PO}_3\text{H})_2$ ^f	Site 1 (P1)	(1Ca; 2Ca; 1H)		37.1		54.9		0.88
	Site 2 (P2)	(1Ca; 2Ca; 1H)		39.7		56.5		0.80
Ca-EDTMP ^g	Site 1 (P1)	(1Ca, 1H, /)		16.1		98.9		0.83
	Site 2 (P2)	(1Ca, 1H, /)		16.7		-120.8		0.76
Ca-CEPA ^h	(1Ca, 1Ca, 2Ca)		33.4		52.7		0.62	
$\text{Ca}_3(\text{HPAA})_2(\text{H}_2\text{O})_{14}$ ⁱ	(1Ca, /, /)		27.0		74.0		0.15	
Ca-PMIDA ^j	(1Ca, 1Ca, 1H)		9.8		-91.5		0.88	

^a Connectivity determined using $d(\text{Ca}\dots\text{O}) = 3 \text{ \AA}$ as a cut-off.

^b Experimental values were obtained at ~25°C.

^c Error bars on the experimental values were determined from the fitting of 2 independent ^{31}P NMR spectra (either 2 MAS recorded at different speeds and magnetic field, or 1 MAS and 1 static).

^d NMR parameters were calculated on structural models after relaxation of all atomic positions.

^e The principal values δ_{11} , δ_{22} and δ_{33} are sorted such as $|\delta_{33} - \delta_{\text{iso}}| \geq |\delta_{11} - \delta_{\text{iso}}| \geq |\delta_{22} - \delta_{\text{iso}}|$. Then, $\delta_{\text{iso}} = 1/3(\delta_{11} + \delta_{22} + \delta_{33})$, $\Delta_{\text{CS}} = \delta_{33} - \delta_{\text{iso}}$, and $\eta_{\text{CS}} = (\delta_{22} - \delta_{11})/(\delta_{33} - \delta_{\text{iso}})$.

^f Mallouk *et al*, *Inorg. Chem.*, 1990, **29**, 2112; (CSD SEZVOI and SEZVUO).

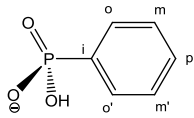
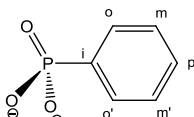
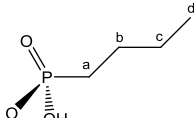
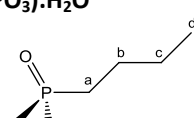
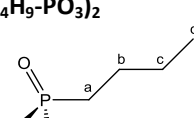
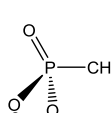
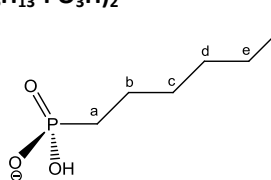
^g Demadis *et al*, *Cryst. Growth Design*, 2009, **9**, 1250; (CCDC 605561).

^h Demadis *et al*, *Appl. Mater. Interf.*, 2009, **1**, 35; (CCDC 607002).

ⁱ Demadis *et al*, *Appl. Mater. Interf.*, 2010, **2**, 1814; (CCDC 766599).

^j Stavgianoudaki *et al*, *Cryst. Eng. Comm.*, 2012, **14**, 5385; (CCDC 870777).

Table S7. Experimental and calculated ^{13}C isotropic chemical shifts.

	C type ^a	C number ^b	δ_{iso} (ppm)		$J_{\text{P-C}}$ (Hz) Exp	
			Exp ^{c,d}	Calc ^d		
Ca(C₆H₅-PO₃H)₂ 	C _i	C ₁	135.2	139.0	¹ J _{P-C} = 195 ± 10 ^f	
	C _o	C ₆	134.0	137.0		
	C _{o'}	C ₂	131.3	134.4		
	C _m	C ₄	} ~127.9 ^e	131.1		
	C _{m'}	C ₅		130.5		
	C _p	C ₃		129.3 ^e		129.6
	Ca(C₆H₅-PO₃)₂·2H₂O 	C _i	C ₅	138.4 ^e		141.2
C _o		C ₆	} 127 to 133	134.6		
C _{o'}		C ₇		134.8		
C _m		C ₈		132.6		
C _{m'}		C ₉		131.5		
C _p		C ₁₀		129.8 ^e	134.8	
Ca(C₄H₉-PO₃H)₂ 		C _a	C ₄	31.9 ^g	31.5	¹ J _{P-C} = 140 ± 2
	C _b	C ₃	27.9 ^g	27.2		
	C _c	C ₂	~27.9 ^g	26.6	¹ J _{P-C} = 140 ± 2	
	C _d	C ₁	16.3 ^g	14.4		
	C _{a'}	C ₁₂	30.1 ^h	29.3		
	C _{b'}	C ₁₁	28.7 ^h	26.9		
	C _{c'}	C ₁₀	~27.9 ^h	25.8		
	C _{d'}	C ₉	15.9 ^h	14.2		
	Ca(C₄H₉-PO₃)₂·H₂O 	C _a	C ₂	30.0 ^e	29.7	¹ J _{P-C} = 137 ± 2
		C _b	C ₃	28.2 ^e	26.3	
C _c		C ₄	26.2 ^e	25.5	³ J _{P-C} = 13 ± 2 ⁱ	
C _d		C ₅	15.2 ^e	12.5		
Ca_{1.5}Na(C₄H₉-PO₃)₂ 		C _a	/	31.5 ^j		/
	C _b	/	29.1 ^j	/		
	C _c	/	26.2 ^j	/	³ J _{P-C} = 15 ± 2 ⁱ	
	C _d	/	15.2 ^j	/		
	C _{a'}	/	29.6 ^k	/	¹ J _{P-C} = 134 ± 2	
	C _{b'}	/	27.7 ^k	/		
	C _{c'}	/	25.1 ^k	/	³ J _{P-C} = 19 ± 2 ⁱ	
	C _{d'}	/	14.0 ^k	/		
Ca(CH₃-PO₃)₂·H₂O^l 	C	C ₁	/	14.6		
Ca(C₆H₁₃-PO₃H)₂^l 	C _a	C ₁	/	32.5		
	C _b	C ₂	/	26.1		
	C _c	C ₃	/	37.1		
	C _d	C ₄	/	35.5		
	C _e	C ₅	/	27.3		
	C _f	C ₆	/	14.6		
	C _a	C ₇	/	29.5		
	C _b	C ₈	/	27.2		
	C _c	C ₉	/	35.9		
	C _d	C ₁₀	/	36.0		
	C _e	C ₁₁	/	26.0		
	C _f	C ₁₂	/	14.1		

^a The "C type" designates the positioning of the C atom along the phosphonate chain, as depicted on the figures on the left.

^b The "C number" provides the numbering of the C atoms in the corresponding .cif file.

^c The experimental ¹³C chemical shifts correspond to spectra recorded +10 °C. Maximum error bars on experimental ¹³C chemical shifts: ± 0.3 ppm for phenylphosphonates; ± 0.2 ppm for butylphosphonates.

^d Calculated values correspond to structural models after relaxation of all atomic positions.

^e Assignment proposed on the basis of ¹³C{³¹P} REDOR experiments.

^f The ¹J_{P-C} we measured in the case of the related Sr(C₆H₅-PO₃H)₂ phase is also ~195 Hz (data not shown).

^g Butyl chain attached to the P at δ_{iso}(³¹P) = 25.3 ppm; assignment of the peaks on the basis of ¹³C{³¹P} REDOR and ¹H-¹³C-³¹P double-CP experiments.

^h Butyl chain attached to the P at δ_{iso}(³¹P) = 26.8 ppm; assignment of the peaks on the basis of ¹³C{³¹P} REDOR and ¹H-¹³C-³¹P double-CP experiments.

ⁱ ³J_{P-C} values were determined from CPMAS spectra recorded at 14.1 T and spinning at 20 kHz MAS (with no temperature regulation). (see figure S16)

^j Butyl chain attached to the P at δ_{iso}(³¹P) = 23.1 ppm; assignment of the peaks on the basis of ¹³C{³¹P} REDOR and ¹H-¹³C-³¹P double-CP experiments.

^k Butyl chain attached to the P at δ_{iso}(³¹P) = 25.8 ppm; assignment of the peaks on the basis of REDOR and ¹H-¹³C-³¹P double-CP experiments.

^l Mallouk *et al*, *Inorg. Chem.*, 1990, **29**, 2112; (CSD SEZVOI and SEZVUO).

Table S8. Experimental and calculated ^{43}Ca NMR parameters.

	δ_{iso} (ppm)		C_Q (MHz)		η_Q	
	Exp ^{a,b}	Calc ^{c,d}	Exp ^{a,b,e}	Calc ^c	Exp ^{a,b}	Calc ^c
$\text{Ca}(\text{C}_6\text{H}_5\text{-PO}_3\text{H})_2$	-14 ± 4	-20.0	3.5 ± 0.6	2.3	0.4 ± 0.3	0.5
$\text{Ca}(\text{C}_6\text{H}_5\text{-PO}_3)\cdot 2\text{H}_2\text{O}$	17.9 ± 0.4	18.2	3.09 ± 0.07	2.1	0.75 ± 0.10	0.7
$\text{Ca}(\text{C}_4\text{H}_9\text{-PO}_3\text{H})_2$	0 ± 4	-5.1	2.78 ± 0.20	1.6	0.6 ± 0.3	0.9
$\text{Ca}(\text{C}_4\text{H}_9\text{-PO}_3)\cdot \text{H}_2\text{O}$	17 ± 1	16.9	2.49 ± 0.02	1.4	0.5 ± 0.1	0.5
$\text{Ca}_{1.5}\text{Na}(\text{C}_4\text{H}_9\text{-PO}_3)_2$	Site 1	30.4 ± 0.4	1.55 ± 0.09		0.6 ± 0.1	
	Site 2	2 ± 2	2.25 ± 0.25		0.75 ± 0.20	
$\text{Ca}(\text{CH}_3\text{-PO}_3)\cdot \text{H}_2\text{O}$ ^f		21.8		1.5		0.6
$\text{Ca}(\text{C}_6\text{H}_{13}\text{-PO}_3\text{H})_2$ ^f		2.2		1.9		0.8
Ca-EDTMP ^g		47.0		1.6		0.7
Ca-CEPA ^h		12.4		0.7		0.3
$\text{Ca}_3(\text{HPAA})_2(\text{H}_2\text{O})_{14}$ ⁱ	Site 1	31.9		2.2		0.6
	Site 2	2.7		-1.0		0.7
Ca-PMIDA ^j		18.1		2.0		0.7

^a Experimental values were obtained at $\sim 25^\circ\text{C}$.

^b Error bars were determined from simultaneous simulations of the ^{43}Ca NMR spectra recorded at 14.1 and 20.0 T.

^c NMR parameters were calculated on structural models after relaxation of all atomic positions.

^d The error on calculated ^{43}Ca isotropic chemical shifts is generally estimated to 5 ppm.

^e The sign of C_Q is not measured experimentally.

^f Mallouk *et al*, *Inorg. Chem.*, 1990, **29**, 2112 ; (CSD SEZVOI and SEZVUO).

^g Demadis *et al*, *Cryst. Growth Design*, 2009, **9**, 1250 ; (CCDC 605561).

^h Demadis *et al*, *Appl. Mater. Interf.*, 2009, **1**, 35 ; (CCDC 607002).

ⁱ Demadis *et al*, *Appl. Mater. Interf.*, 2010, **2**, 1814 ; (CCDC 766599).

^j Stavgianoudaki *et al*, *Cryst. Eng. Comm.*, 2012, **14**, 5385 ; (CCDC 870777).

Table S9. Experimental and calculated ^1H isotropic chemical shifts.

	H type ^a	H number ^b	δ_{iso} (ppm)	
			Exp ^c	Calc ^d
Ca(C₆H₅-PO₃H)₂	O-H	H ₁₆	~12.2	13.2
		H_{ar}		H ₁₁
	H ₁₂			7.0
	H ₁₃			5.2
	H ₁₄			6.2
	H ₁₅			7.4
Ca(C₆H₅-PO₃).2H₂O	O-H	H ₁₉	~2.6 (1.6 to 3.4)	2.2
		H ₂₀		3.0
		H ₂₁		3.7
	H_{ar}	H ₂₂	5.4 to 8.0	8.8
		H ₁₁		6.2
		H ₁₂		7.8
		H ₁₃		6.4
		H ₁₄		7.2
		H ₁₅		7.1
Ca(C₄H₉-PO₃H)₂	O-H	H ₃₆	~10.6	11.7
		H_{bu}		H ₃₇
	H ₁₈			0.8
	H ₁₉			1.2
	H ₂₀			0.7
	H ₂₁			1.3
	H ₂₂			1.1
	H ₂₃			1.6
	H ₂₄			1.2
	H ₂₅			1.7
	H ₂₆			2.3
	H ₂₇			0.8
	H ₂₈			1.2
	H ₂₉			0.8
	H ₃₀			1.1
	H ₃₁			1.3
	H ₃₂			1.3
	H ₃₃			1.4
	H ₃₄	2.1		
H ₃₅	1.9			
Ca(C₄H₉-PO₃).H₂O	O-H	H ₂₀	~5.4	6.2
		H_{bu}		H ₂₁
	H ₁₁			2.1
	H ₁₂			2.0
	H ₁₃			1.3
	H ₁₄			1.2
	H ₁₅			0.9
	H ₁₆			1.2
	H ₁₇			0.8
	H ₁₈			0.8
	H ₁₉	1.3		
Ca_{1.5}Na(C₄H₉-PO₃)₂	H_{bu}	/	0.4 to 2.1	/
Ca(CH₃-PO₃).H₂O^e	O-H	H ₄	/	6.2
		H ₅		5.4
	H_{me}	H ₁		1.4
		H ₂		2.0
		H ₃		2.2

Ca(C₆H₁₃-PO₃H)₂ ^e	O-H	H ₁	/	13.4	
		H ₂		12.5	
	H_{hex}		H ₃		1.8
			H ₄		2.6
			H ₅		1.9
			H ₆		1.2
			H ₇		1.3
			H ₈		1.3
			H ₉		1.4
			H ₁₀		1.1
			H ₁₁		1.5
			H ₁₂		1.3
			H ₁₃		1.0
			H ₁₄		0.9
			H ₁₅		1.3
			H ₁₆		2.1
			H ₁₇		2.4
			H ₁₈		1.4
			H ₁₉		1.6
			H ₂₀		1.1
			H ₂₁		1.5
			H ₂₂		1.3
			H ₂₃		1.3
			H ₂₄		1.4
			H ₂₅		1.3
			H ₂₆		1.3
			H ₂₇		1.0
			H ₂₈		0.9

^a The "H type" differentiates H atoms bound to a C atom of the organic chain from those bound to an O atom (belonging to a water molecule or phosphonate).

^b The "H number" provides the numbering of the H atoms in the corresponding .cif file.

^c Experimental values were obtained at ~25°C.

^d NMR parameters were calculated on structural models after relaxation of all atomic positions.

^e Mallouk *et al*, *Inorg. Chem.*, 1990, **29**, 2112 ; (CSD SEZVOI and SEZVUO).